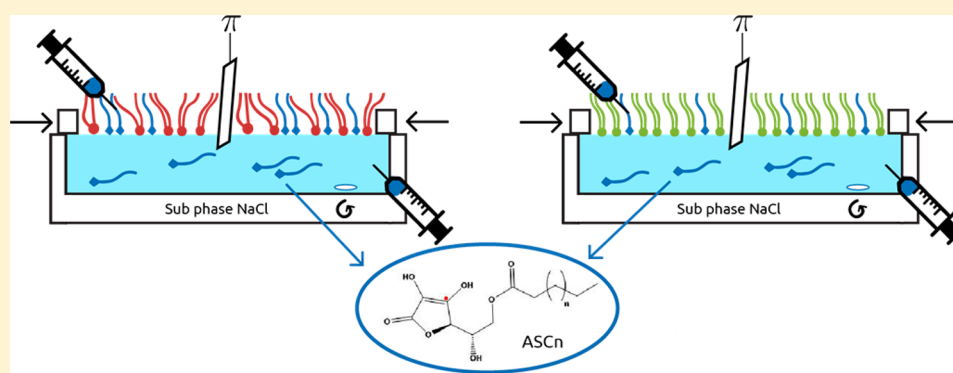


# The Rheological Properties of Lipid Monolayers Modulate the Incorporation of L-Ascorbic Acid Alkyl Esters

Yenisleidy de las Mercedes Zulueta Díaz,<sup>†</sup> Milagro Mottola,<sup>†</sup> Raquel V. Vico,<sup>‡</sup> Natalia Wilke,<sup>†</sup> and María Laura Fanani<sup>\*,†</sup>

<sup>†</sup>Centro de Investigaciones en Química Biológica de Córdoba (CIQUIBIC–CONICET), Departamento de Química Biológica and, <sup>‡</sup>Instituto de Investigaciones en Físicoquímica de Córdoba (INFIQC–CONICET), Departamento de Química Orgánica, Facultad de Ciencias Químicas, Universidad Nacional de Córdoba. Haya de la Torre y Medina Allende, Ciudad Universitaria, X5000HUA, Córdoba, Argentina

## S Supporting Information



**ABSTRACT:** In this work, we tested the hypothesis that the incorporation of amphiphilic drugs into lipid membranes may be regulated by their rheological properties. For this purpose, two members of the L-ascorbic acid alkyl esters family ( $ASC_n$ ) were selected,  $ASC_{16}$  and  $ASC_{14}$ , which have different rheological properties when organized at the air/water interface. They are lipophilic forms of vitamin C used in topical pharmacological preparations. The effect of the phase state of the host lipid membranes on  $ASC_n$  incorporation was explored using Langmuir monolayers. Films of pure lipids with known phase states have been selected, showing liquid-expanded, liquid-condensed, and solid phases as well as pure cholesterol films in liquid-ordered state. We also tested ternary and quaternary mixed films that mimic the properties of cholesterol containing membranes and of the stratum corneum. The compressibility and shear properties of those monolayers were assessed in order to define its phase character. We found that the length of the acyl chain of the  $ASC_n$  compounds induces differential changes in the rheological properties of the host membrane and subtly regulates the kinetics and extent of the penetration process. The capacity for  $ASC_n$  uptake was found to depend on the phase state of the host film. The increase in surface pressure resultant after amphiphile incorporation appears to be a function of the capacity of the host membrane to incorporate such amphiphile as well as the rheological response of the film. Hence, monolayers that show a solid phase state responded with a larger surface pressure increase to the incorporation of a comparable amount of amphiphile than liquid-expanded ones. The cholesterol-containing films, including the mixture that mimics stratum corneum, allowed a very scarce  $ASC_n$  uptake independently of the membrane diffusional properties. This suggests an important contribution of Cho on the maintenance of the barrier function of stratum corneum.

## 1. INTRODUCTION

L-ascorbic acid alkyl esters ( $ASC_n$ ) are lipophilic forms of vitamin C (see Scheme 1). They are drugs with pharmacological interest due to their antioxidant properties and amphiphilic behavior.<sup>1,2</sup> The presence of the acyl chain, besides improving their solubility in alcohol and nonpolar solvents, provides the capacity to self-organize into monolayer films when are placed at the air–water interface<sup>3,4</sup> as well as into micelles and coagel when are suspended in water.<sup>1,5</sup> These characteristics enable them to constitute a promising tool as drug carriers in pharmaceutical dosage formulations because

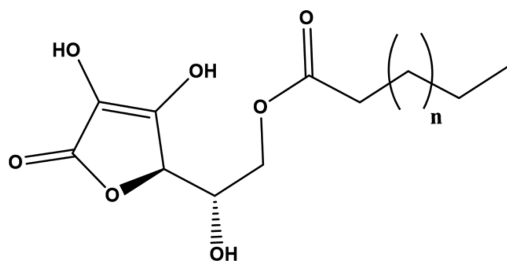
they enhance the skin and ocular permeation,<sup>6,7</sup> as well as in new adjuvant preparations<sup>8</sup> and liposome-based drug delivery systems.<sup>9</sup> Additionally, it has been recently reported that some members of this drug family present bactericidal and antileishmanial activity.<sup>10</sup>

Despite the widespread use of  $ASC_n$  in cosmetology and dermatology, there is still lack of information about the

Received: November 12, 2015

Revised: December 21, 2015

Published: December 22, 2015

Scheme 1. Chemical Structure of ASC<sub>n</sub><sup>a</sup>

<sup>a</sup>"n" stands for 12 (ASC<sub>16</sub>) or 10 (ASC<sub>14</sub>).

physicochemical basis of their interaction with membranes, which is of relevance because the cell membranes are the first contact area of lipophilic drugs with cells. We recently studied the surface behavior of ASC<sub>n</sub> with acyl chains of different lengths (C16, C14 and C12, namely ASC<sub>16</sub>, ASC<sub>14</sub>, and ASC<sub>12</sub>, respectively), which exhibited good surface activity forming Gibbs monolayers. They were also able to penetrate into closely packed phospholipid monolayers.<sup>4</sup>

In a former work, we also explored the penetration of ASC<sub>16</sub> into mixed monolayers composed of phosphatidylcholine/cholesterol (Cho). The formation of the liquid-ordered (LO) phase, characteristic of a Cho-containing membrane favored the insertion kinetics of ASC<sub>16</sub><sup>5</sup> suggesting a fundamental roll of the rheological properties of the biomembranes. When an amphiphilic molecule inserts into a biomembrane, it exerts an in-plane compression causing a lateral displacement of the other components of the membrane so that lateral pressure opposes the incorporation. Then the ability of the lipidic film to respond to an isometric compression/expansion (compressibility) and to a lateral displacement (in-plane diffusion) of the components may condition the insertion of a new molecule into the membrane.

Because the ASC<sub>n</sub> family has been mainly used in topical pharmacological preparations, it is relevant the question of how these amphiphilic drugs are incorporated into a particular tissue, the stratum corneum, where the biological function is highly controlled by the lipid composition.<sup>11,12</sup> Several reports<sup>13,14</sup> have proposed that model membranes composed of Cho, ceramide (Cer), long chain fatty acids with or without incorporation of cholesterol sulfate (ChoS) closely mimic the stratum corneum structure and its barrier function. Of those key components, long chain fatty acids and Cers typically form liquid-condensed (LC) or solid (S) Langmuir monolayers with high shear modulus<sup>15–18</sup> while Cho typically provides a LO character.<sup>19</sup> A detailed analysis of the surface structure and compressibility of Langmuir monolayers composed of a quaternary lipid mixture that mimic stratum corneum lipid composition has provided evidence of a solid phase.<sup>20,21</sup> Therefore, the following questions arise: how amphiphilic drugs (like ASC<sub>n</sub>) are incorporated into such solid membrane? What are the differences in the penetration of these drugs in membranes with different rheological conditions? Do the ASC<sub>n</sub> molecules alter the rheological properties of the membrane after their incorporation?

A comprehensive literature search provides little amount of information about the influence of the phase state of biomembranes on its ability of incorporating amphiphilic drugs.<sup>22–26</sup> In this work, we explored the modulation of ASC<sub>n</sub> incorporation into model membrane systems by their rheological properties. The ability of drug incorporation by the

quaternary lipid mixture that mimics several aspects of the stratum corneum barrier was also tested. Two ASC<sub>n</sub> members were selected for this study, ASC<sub>16</sub> and ASC<sub>14</sub>, which have different rheological properties when organized at the air/saline solution interface by themselves. At a neutral pH, ASC<sub>16</sub> forms an LC phase at relatively high- $\pi$  while ASC<sub>14</sub> forms a liquid-expanded (LE) phase in the whole  $\pi$  range.<sup>4</sup>

In this context, a deep knowledge of the interactions between ASC<sub>n</sub> and lipidic model membranes with different rheological character will allow us to gain significant insight about the principles of selectivity of these drugs for each membrane type.

## 2. EXPERIMENTAL SECTION

Commercial 6-*O*-palmitoyl-*L*-ascorbic acid (ASC<sub>16</sub>) was supplied by Sigma and exhaustively purified as described in ref 4. 6-*O*-Myristic-*L*-ascorbic acid (ASC<sub>14</sub>) was synthesized and purified as described in ref 4.

1-palmitoyl-2-oleoyl-*sn*-glycero-3-phosphocholine (POPC), 1, 2-distearoyl-*sn*-glycero-3-phosphocholine (DSPC), *N*-palmitoyl-*D*-erythro-sphingosylphosphorylcholine (SM16), cholesterol (Cho) and (d18:1/24:0)*N*-lignoceroyl-*D*-erythro-sphingosine (Cer24) were purchased from Avanti Polar Lipids, Inc. (Alabama, U.S.A.). Lignoceric acid (LA) and cholesterol-3-sulfate sodium salt (ChoS) as well as micrometer-sized beads (3  $\mu$ m diameter, polystyrene LB30) were provided by SIGMA. All other reagents were of analytical grade (99% pure) and used without further purification. The water was purified by a Milli-Q (Millipore, Billerica, MA) system to yield a product with a resistivity of  $\sim$ 18.5 M $\Omega$ .

The mixed monolayers used were cholesterol-containing membranes (CCM) composed of POPC/SM16/Cho (25:25:50) and stratum corneum mimicking membrane (SCM) composed of Cer24/LA/Cho 33:33:33 with addition of 5% w/w ChoS.

Lipid monolayers were prepared and characterized in a Langmuir film balance with isometric compression as detailed before<sup>16</sup> onto NaCl 145 mM (pH  $\sim$  6.5) subphase at (25  $\pm$  1) °C. Compression isotherms reported as surface pressure ( $\pi$ ) versus mean molecular area (MMA) plots were obtained from monolayers of pure lipids (POPC, SM16 DSPC and Cho) and lipid mixtures.<sup>20</sup>

Studies of the lipid film properties were performed as detailed in the Supporting Information (SI). Briefly, the mechanical properties were evaluated through the compressibility modulus (from compression isotherms, see Section 1 of SI and ref 27) and the diffusion coefficient of latex microspheres inserted in the Langmuir monolayer (see ref 28 and Section 2 of SI). Langmuir monolayers were also visualized in the microscale by Brewster angle microscopy (see Section 3 of SI) in order to evaluate the phase coexistence and domains shape.<sup>16,29,30</sup> ASC<sub>n</sub> penetration into lipid monolayers has been evaluated as previously reported<sup>5</sup> and detailed in Section 4 of SI. Those experiments were performed by injecting an amount of drug solution into the subphase of a preformed lipid film and registering the increase of  $\pi$  as a function of time. From the results of penetration experiments and compression isotherms, the mole fraction of drug incorporated into the lipid monolayer after reaching the equilibrium  $\pi$  was estimated as detailed in Section 5 of SI.

## 3. RESULTS AND DISCUSSION

### 3.1. Rheological Properties of the Tested Lipid Monolayers.

In this work, we explored the interaction of ASC<sub>n</sub> with lipid monolayers showing different phase states. For this purpose, we used monolayers of pure lipids, which display well-defined and known phase states such as POPC, SM16, and DSPC<sup>27,28,31,32</sup> and pure Cho films. Compression isotherms of such monolayers (Figure 1) show characteristics of LE, LC, and S at  $\pi \geq 30$  mN/m, respectively (SM16 also undergoes an LE to LC phase transition at  $\sim$ 17 mN/m) accordingly to bibliographic data.<sup>27,28,31,32</sup>

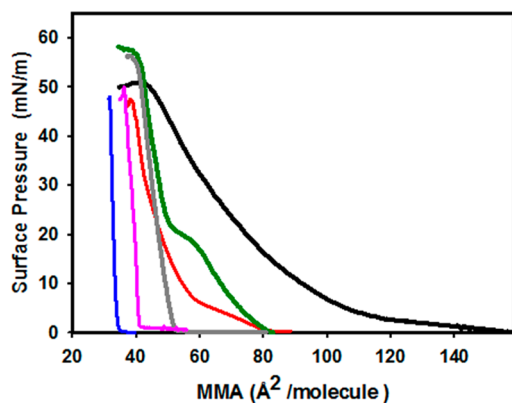


**Figure 1.** Isothermal compression of Langmuir monolayers of the studied lipids. The curves are representative experiments, which vary by less than 2 mN/m from their corresponding replicas. The membranes studied were composed of POPC (black), SM16 (green), DSPC (gray), Cho (magenta), CCM (red), and SCM (blue).

The assignment of a phase state to a lipid monolayer has been usually based on the study of its elastic response upon a dilatational stress (i.e., the compressibility modulus).<sup>33</sup> For LE monolayers (like those formed by POPC), a decrease in the available area induces a relatively low increase in  $\pi$ , resulting in low compressibility modulus ( $C_s^{-1}$ ) values, typically  $<100$  mN/m.<sup>33</sup> For LC and S monolayers, a larger increase in  $\pi$  is induced by a small reduction of the monolayer area, leading to  $C_s^{-1}$  values several folds higher than for POPC monolayers (Table 1).

Early studies have reported compression isotherms of pure Cho monolayers as highly incompressible films<sup>27</sup> (with high  $C_s^{-1}$  values, see Table 1), which have been described in the 60th as “rather condensed films”.<sup>33</sup> Lately, liquid–liquid phase coexistence was visualized by fluorescence microscopy in Cho-containing monolayers.<sup>34,35</sup>

Pioneer studies reported that Cho introduces a liquefier effect into phospholipid monolayers<sup>36</sup> and in agreement with that more recent studies evidenced that Cho-containing monolayers behave as viscous fluids,<sup>18</sup> which correlates with early studies that assign a fluid character to Cho-containing bilayers.<sup>12</sup> Then, by analogy with the liquid-ordered phase (LO) reported for bilayers containing high amount of Cho<sup>37,38</sup> the thicker Cho-enriched liquid-phase in coexistence with the LE phase found in monolayers was also named LO phase.<sup>18,19</sup>

In the present work, we tested the shear viscosity properties of different lipid monolayers including pure Cho films.

The diffusion of the beads at a modified air–water interface will depend on the contact angle, on water viscosity, on the percent of the sphere that is sunk, and on the surface viscosity.<sup>39,40</sup> From one monolayer to another, it is expected mostly to change this last parameter and thus, a comparison of the diffusion of the beads ( $D$ ) in the different monolayers provides an indirect manner of comparing the shear viscosity of the films.

Figure 2 shows the mean square displacement (MSD) of latex beads inserted in different lipid monolayers as a function

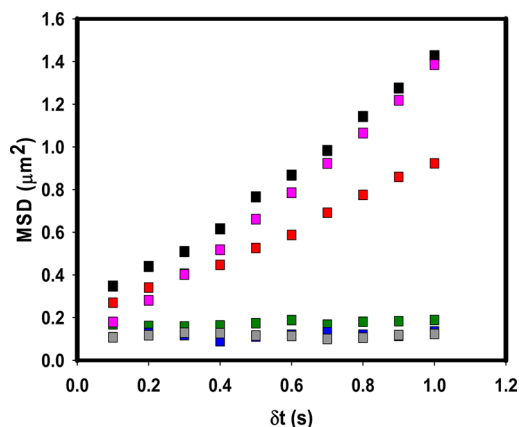


**Figure 2.** Tracking of single particles of latex beads on different monolayers. Relative MSD versus time intervals ( $\Delta t$ ) for  $3 \mu\text{m}$  beads in lipid monolayers at 30 mN/m. The data corresponds to representative experiments. From the analysis of 40 such trajectories, statistical data of  $D$  was calculated for each lipid film and reported in Table 1. The monolayers studied were composed of POPC (black), SM16 (green), DSPC (gray), Cho (magenta), CCM (red), and SCM (blue).

of time interval. From the slope of these curves and after eq S2 in Supporting Information (see ref 28)  $D$  was calculated. It is clear that DSPC and SM16 films (S and LC phases) have a severely restricted lateral diffusion (compared with monolayers composed of POPC and Cho) giving  $D$  values below  $1 \times 10^{-2} \mu\text{m}^2/\text{s}$  (see Table 1), which match with the values reported in the literature for LC monolayer ( $1 \times 10^{-4}$  to  $5 \times 10^{-3} \mu\text{m}^2/\text{s}$ , see ref 28). LE monolayers composed of POPC presented  $D$  values similar than that for Cho films (in the order of  $10^{-1} \mu\text{m}^2/\text{s}$ ), evidencing a low shear viscosity for both monolayers.

**Table 1. Properties of Lipid Monolayers at 30 mN/m and Their Capacity to Incorporate  $\text{ASC}_n$**

lipid composition	rheological characterization of the lipid monolayers			$\text{ASC}_n$ incorporation into monolayers					
				$\pi$ increase (mN/m) <sup>d</sup>		$X_{90}$		Estimated $X_{\text{ASC}_n}^{\text{req}}$ <sup>e</sup>	
	$C_s^{-1}$ (mN/m) <sup>a</sup>	$D$ ( $\mu\text{m}^2/\text{s}$ ) <sup>b</sup>	phase state <sup>c</sup>	$\text{ASC}_{16}$	$\text{ASC}_{14}$	$\text{ASC}_{16}$	$\text{ASC}_{14}$	$\text{ASC}_{16}$	$\text{ASC}_{14}$
POPC	$83 \pm 9$	$0.3 \pm 0.2$	LE	$13 \pm 1$	$14 \pm 1$	$0.30 \pm 0.03$	$0.52 \pm 0.02$	$0.38 \pm 0.04$	$0.39 \pm 0.04$
SM16	$162 \pm 29$	$< 1 \times 10^{-2}$	LC	$19 \pm 1$	$18 \pm 1$	$0.27 \pm 0.02$	$0.41 \pm 0.08$	$0.20 \pm 0.02$	$0.20 \pm 0.02$
DSPC	$257 \pm 20$	$< 1 \times 10^{-2}$	S	$26 \pm 2$	$27 \pm 1$	$0.09 \pm 0.01$	$0.10 \pm 0.01$	$0.18 \pm 0.02$	$0.18 \pm 0.02$
Cho	$358 \pm 37$	$0.2 \pm 0.1$	LO	$16 \pm 1$	$18 \pm 1$	$0.04 \pm 0.01$	$0.07 \pm 0.02$	$0.09 \pm 0.01$	$0.09 \pm 0.01$
CCM	$142 \pm 7$	$(6 \pm 3) \times 10^{-2}$	LO	$17 \pm 1$	$15 \pm 1$	$0.05 \pm 0.01$	$0.07 \pm 0.01$	$0.18 \pm 0.02$	$0.17 \pm 0.02$
SCM	$272 \pm 40$	$< 1 \times 10^{-2}$	LC	$17 \pm 1$	$16 \pm 1$	$0.04 \pm 0.01$	$0.05 \pm 0.01$	$0.03 \pm 0.01$	$0.03 \pm 0.01$

<sup>a</sup>Evaluated at 30 mN/m. Error represent SEM of 2–3 independent experiments. <sup>b</sup>Evaluated at 30 mN/m. Error represent SD of 40 individual trajectories analyzed from 3 independent experiments. Calculated after eq S2 in Supporting Information. <sup>c</sup>Phase state estimated for lipid films based on  $C_s^{-1}$ ,  $D$  and microscopy data (Figure 3). <sup>d</sup> $\pi$  increase after penetration of  $\text{ASC}_n$  into a preformed lipid monolayer at 30 mN/m (taken from data in Figure 4B). <sup>e</sup>Estimated after eq S5 in Supporting Information.

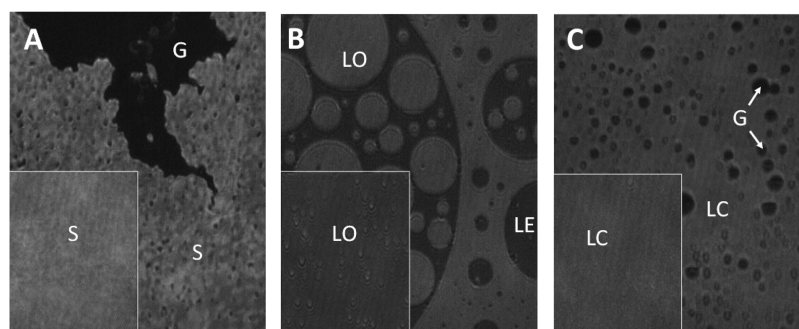


**Figure 3.** Brewster angle microscopy images of monolayers composed of pure DSPC (A), Cho-containing membrane (CCM) (B), and SCM (C). Images were obtained at low  $\pi$  ( $<1$  mN/m). Insets show the same films at 30 mN/m. The pictures are representative of 5–7 images from two independent experiments. For a better visualization, a lower gray level range was selected (range of 0–80 from a 0–255 original scale). The letters refers to the phase state of the film: G, LE, LO, LC, and S. Main Images are  $250 \times 200 \mu\text{m}$  and insets are  $125 \times 100 \mu\text{m}$ .

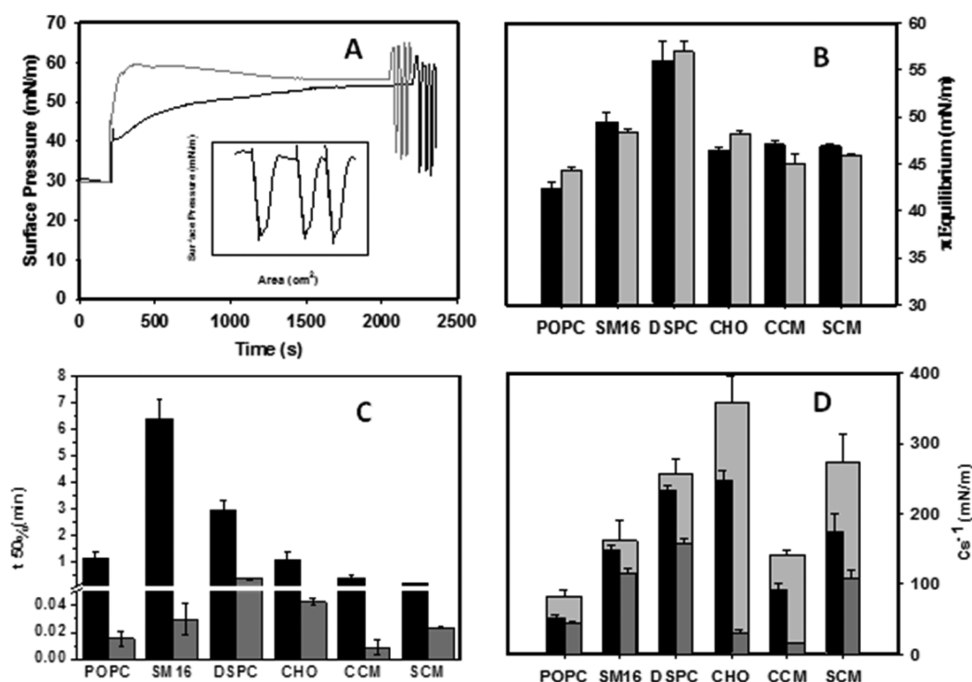


**Figure 4.** Penetration of  $\text{ASC}_{14}$  and  $\text{ASC}_{16}$  into monolayers with different rheological character at 30 mN/m. (A) Representative penetration curve showing the insertion of  $\text{ASC}_{16}$  (black line) or  $\text{ASC}_{14}$  (gray line) into pure DSPC monolayers. (B)  $\pi_{\text{eq}}$  values achieved after insertion of  $\text{ASC}_n$  to the acceptor monolayers. (C) Insertion kinetics of  $\text{ASC}_n$  in the acceptor monolayer expressed as  $t_{50\%}$ . Bars in (B,C) represent values after insertion of  $\text{ASC}_{16}$  (black) or  $\text{ASC}_{14}$  (gray). (D) Comparison of the mean values of compressibility modulus ( $\text{Cs}^{-1}$ ) of monolayers in the absence (light gray bars) and after equilibration with  $\text{ASC}_n$  in the subphase (black bars corresponds to  $\text{ASC}_{16}$  and dark gray to  $\text{ASC}_{14}$ ); initial surface pressure: 30 mN/m. The error bars corresponds to Standard Error of the Mean. The inset in panel A shows the consecutive compression/expansion of a representative monolayer after  $\text{ASC}_n$  insertion. The  $\text{Cs}^{-1}$  values obtained from the slope of the compression portion are plotted in panel D.

This result agrees with early reports that assign a more viscous character to monolayers of DSPC than Cho.<sup>36</sup> Then, a LO character can be assigned to pure Cho monolayer based on its low compressibility (high  $\text{Cs}^{-1}$ ) and high lateral mobility (Table 1). The results obtained for this film are hardly extrapolated to bilayer systems because pure Cho do not form lamellar structures. Then, a ternary mixture containing POPC/SM16/Cho (1:1:2), which has been assigned as forming LO phases both in bilayer and in monolayer systems<sup>18,19,41</sup> was also studied. This ternary mixture has been used as a model for liquid–liquid domain coexistence and has been of general interest in the past two decades since LO domains have been proposed to occur in living cells.<sup>42</sup> Figure 1 shows the compression isotherm of this “Cho containing membrane” or CCM. This monolayer showed LE–LO phase coexistence by

Brewster angle microscopy (BAM) at  $\pi \leq 6$  mN/m and a homogeneous phase above this value (Figure 3B). A kink in the compression curve can be observed at the two-phases to one-phase transition.

Our rheological analysis for CCM showed lower  $\text{Cs}^{-1}$  values than pure Cho but still higher than those obtained for LE monolayers at 30 mN/m (Table 1),<sup>19</sup> though keeping a high diffusion capacity (Figure 2 and Table 1).

Both LC and S phases show low compressibility (high  $\text{Cs}^{-1}$  values)<sup>33</sup> and a restricted lateral diffusion (Table 1). However, LC phases are liquid phases with viscoelastic character upon shear.<sup>18</sup> Thus, in the presence of coexistence with a more fluid phase (such as LE phases) the LC phases form rounded or flower-like domains in order to balance intradomain repulsion/line tension forces<sup>43</sup> (as has been also observed for SM16



domains).<sup>44</sup> S phases are characterized by a regular internal structure and high shear modulus<sup>17,18</sup> that restrict the relaxation of the domain borders and are observed in the micron-scale as sharp-edged structures (see DSPC solid phase borders when it is in coexistence with a gas phase (G) in Figure 3A and,<sup>45</sup> and Cer monolayers in ref 16).

Finally, another mixed film has caught our interest: the SCM. This quaternary monolayer (an equimolar mixture of Cer, free fatty acid and Cho, plus 5% w/w of ChoS) has been previously studied by Vavrova and co-workers and found that it contains a high proportion of orthorhombic structure (solid) when transferred to a solid support and analyzed by AFM.<sup>20</sup> We extended this analysis to rheological and structural properties of the monolayer at the air/saline solution interface.

The compression isotherms and diffusional properties of SCM monolayers evidenced an LC behavior (see Table 1). Accordingly, the BAM inspection showed rounded domain borders when in coexistence with a G phase (Figure 3C, low- $\pi$ ), which resembles closely the coexistence of fluid phases (Figure 3B) rather than S-G phases (Figure 3A). Then, at the air/saline solution interface SCM monolayers behave as an LC phase, rather than an S phase, as has been previously proposed for this membrane when organized onto a solid support.<sup>20</sup>

On the other hand, BAM experiments of SCM monolayers at the air/saline solution interface at high  $\pi$  (30 mN/m) appeared as an homogeneous film (Figure 3B), contrary to AFM studies on SCM films transferred to solid supports, where phase coexistence was found.<sup>20,21,46</sup> The difference between previous reports and the results shown here may be due to an stabilization of the more ordered phase, promoted by the solid support.<sup>47</sup> Furthermore, it is possible that phase coexistence were present in SCM monolayers but with very small domains (smaller than BAM resolution, which is  $\sim 0.2$   $\mu\text{m}$ ).

**3.2. Penetration of  $ASC_n$  into Lipid Monolayers of Different Rheological Characteristics.** When  $ASC_{16}$  or  $ASC_{14}$  are injected into the subphase of a saline solution in order to reach a micromolar concentration, part of the molecules self-organizes in bulk lamellar aggregates (see Section 4 in Supporting Information) and part of them are rapidly adsorbed to the bare air/saline solution interface forming Gibbs monolayers, which reach  $\pi \sim 34$ – $37$  mN/m at equilibrium.<sup>4</sup> Those adsorbed monolayers, as well as the formed by surface spreading (Langmuir monolayers at similar  $\pi$ ) showed an LC or LE phase state character for  $ASC_{16}$  or  $ASC_{14}$ , respectively.<sup>4</sup> These drugs are also able to be incorporated into a preformed POPC monolayer, increasing the  $\pi$  when they are injected into the subphase.<sup>4</sup> In the present work, we assessed their capacity to be incorporated into monolayers of different rheological character. For this purpose, penetration experiments were performed (see Figure 4A for a representative experiment).

Figure 4B shows that  $ASC_{16}$  and  $ASC_{14}$  can increase the  $\pi$  of a solid monolayer, such as the formed by pure DSPC from 30 to 55–57 mN/m, which are  $\sim 13$  mN/m larger than when they penetrate into POPC monolayers. The  $\pi$ -values reached after  $ASC_n$  incorporation to DSPC films represents a total  $\pi$  increase of up to 27 mN/m and a lowering of surface tension to values as low as 15 mN/m. In addition, it is worth noting that the equilibrium  $\pi$  ( $\pi_{\text{eq}}$ ) reached for those monolayers were  $\sim 20$  mN/m larger than those reached when  $ASC_n$  are adsorbed to a bare air/saline solution interface.<sup>4</sup>  $ASC_n$  incorporation into pure SM16 monolayers, which form an LC phase, showed an

intermediate behavior between those observed for DSPC and POPC monolayers. On the other hand, when the  $ASC_n$  are incorporated into a fluid monolayer containing Cho (pure Cho and CCM) the  $\pi_{\text{eq}}$  reaches values that were scarcely higher than those obtained with POPC. Notably, the incorporation of  $ASC_n$  into SCM monolayers, which show an LC character (in regard to compressibility and lateral diffusion) resembles the incorporation into the fluid films and did not show the high  $\pi_{\text{eq}}$  observed for solid DSPC monolayers (see Table 1 and Figure 4B).

Figure 4C shows that slower insertion kinetics was observed for condensed or solid monolayers than for fluids ones (note the break in the Y-axis scale), which was quantified by the  $t_{50\%}$  parameter obtained by fitting the  $\pi$  versus time curve with eq S3 (Supporting Information). Additionally,  $ASC_{16}$ , the drug which forms LC monolayers when pure at  $\pi > 25$  mN/m (ref 3) induced a similar  $\pi_{\text{eq}}$  but with larger  $t_{50\%}$  than  $ASC_{14}$  for all the cases studied. The differences observed may be due to the different rheological properties resulting in the drug-enriched monolayer.

To assess how  $ASC_{16}$  and  $ASC_{14}$  alter the film properties when incorporated into the membrane, we compared the  $Cs^{-1}$  parameter of the films before and after reaching  $\pi_{\text{eq}}$  (Figure 4D). The latter  $Cs^{-1}$  values were obtained by compressing/expanding the equilibrated film several times, and calculating the slope of the  $\pi$  versus area plot during each compression (see inset in Figure 4A) using eq S1 (Supporting Information).

Our results indicate that after  $ASC_{14}$  incorporation, the films became more easily compressible for all the monolayers tested but with a notable effect in films that contain Cho (pure Cho, CCM, and SCM). Similar behavior can also be observed for  $ASC_{16}$  but in a lesser extent. This effect may be related to the kinetically favorable insertion of  $ASC_{14}$  compared to  $ASC_{16}$ . The lowering in the condensed character may represent a diminishing in the activation energy required to laterally compress the film in order to place a second molecule of the drug, once the first one is into the film.

To further characterize the penetration of  $ASC_n$  into lipid monolayers, we studied the  $\pi$ -increase after  $ASC_n$  addition into the monolayer subphase, at several initial surface pressures. Figure 5 shows that both  $ASC_{16}$  and  $ASC_{14}$  are incorporated into highly packed lipid monolayers, which correspond to initial surface pressures of up to 45–65 mN/m. The extrapolated maximum  $\pi$  at which each  $ASC_n$  would be able to penetrate (cut off point) has been traditionally taken as an indirect measure of the affinity of amphiphiles to the lipid film.<sup>48</sup>

Our results indicate that  $ASC_{16}$  can be incorporated to SM16 and DSPC (and  $ASC_{14}$  to DSPC) monolayers up to very high surface pressures (58–65 mN/m), while the more fluid membranes incorporate these drugs up to 45–53 mN/m. This trend resembles the behavior observed for the  $\pi_{\text{eq}}$  at 30 mN/m (Figure 4B), another parameter usually taken as an indicator of the amphiphile tendency to insert into membranes. It is worth noting that these cut off values are far higher than the average surface pressure assigned to bilayers membranes (30–35 mN/m, see ref 49 and 50). This suggests that the  $ASC_n$  family is also able to penetrate into lipid bilayers of different rheological character.

**3.3. Estimation the Amount of  $ASC_n$  Incorporated into Lipid Monolayers of Different Rheological Characteristics.** The amount by which  $\pi$  increases as a consequence of the penetration of  $ASC_n$  into the lipid monolayers might depend on at least two factors, (i) the amount of drug

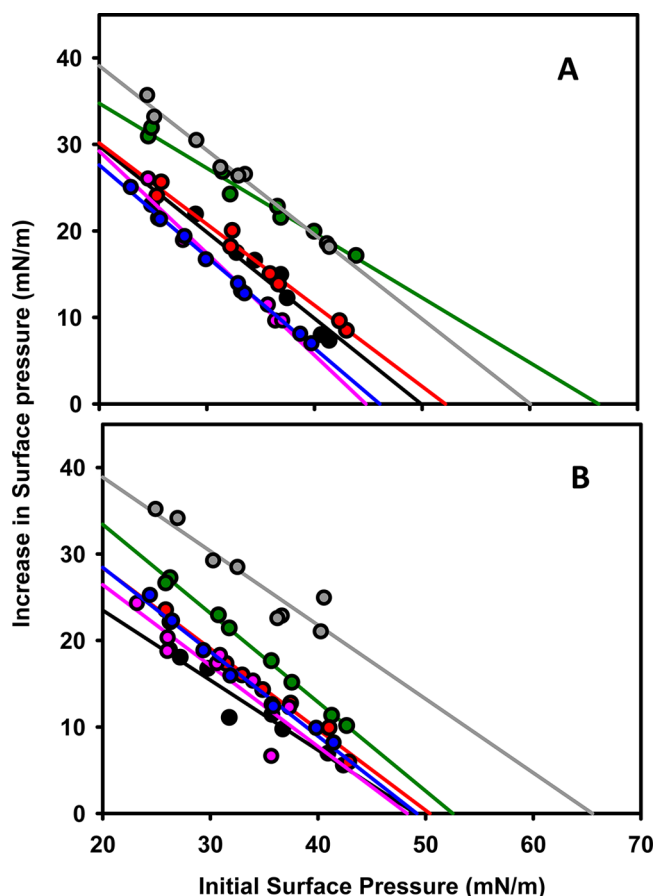


**Figure 5.** Penetration of ASC<sub>16</sub> (A) and ASC<sub>14</sub> (B) into lipid monolayers at different initial packing. The membranes studied are POPC (black), SM16 (green), DSPC (gray), Cho (magenta), CCM (red) and SCM (blue).

incorporated into the lipid film and (ii) the sensibility of the lipid film to the drug incorporation, that is, the mechanical properties of the hosting film. This last factor should be governed by the compression and deformability responses of the acceptor membrane, which was analyzed in the previous section. In order to explain separately both terms, it is necessary to ascertain the capacity of the different lipid films to incorporate these drugs.

We evaluated the ASC<sub>*n*</sub> uptake capacity of lipid monolayers at 30 mN/m by means of surface titration. We spread a known amount of lipids onto the saline solution surface (at constant monolayer area) up to 30 mN/m and then spread stepwise a chloroformic solution of ASC<sub>14</sub> or ASC<sub>16</sub> registering the resultant  $\pi$  increase after solvent evaporation. For all membrane/drug systems studied, a saturating  $\pi$ -value was reached, which did not increase with further addition of drug. Then, we determined the ASC<sub>*n*</sub> mole fraction at which the reached surface pressure was 90% of the saturating pressure ( $X_{90}$ ) (see Figure 6). Our results are summarized in Table 1. As a general rule, ASC<sub>14</sub> was incorporated up to a larger proportion than ASC<sub>16</sub>, and this in turn depended on the rheological properties of the lipid film.

Taking our results together we can observe that the Cho-free monolayers resulted in an increasing condensed character in the order POPC < SM16 < DSPC (LE < LC < S), which was evidenced by an increase in  $C_s^{-1}$  and a decrease in the lateral mobility (D) (Table 1), as expected from literature.<sup>28,31,32</sup> This

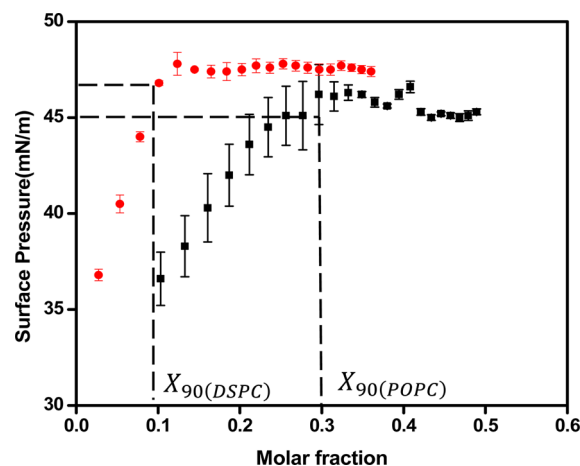


**Figure 6.** Surface titration of lipid monolayers by ASC<sub>*n*</sub> addition. Representative curves of the surface pressure reached after stepwise addition of ASC<sub>16</sub> into initially pure DSPC (red symbols) or POPC (black symbols) at 30 mN/m as a function of the resultant mole fraction of ASC<sub>16</sub>. The dashed lines illustrate the mole fraction necessary to reach 90% of the saturation  $\pi$  ( $X_{90}$ ).

correlated with a decreasing ASC<sub>*n*</sub> uptake capacity: POPC could incorporate ASC<sub>*n*</sub> up to 30–52 mol % before reaching a surface pressure corresponding to 90% of the saturation point, while DSPC could only incorporate <10 mol %. SM16 showed an intermediate behavior for all these parameters.

On the other hand, we performed an estimation of the amount of drug incorporated into the lipid film for penetration experiments using the data obtained from the isotherms (Figure 1 and ref 4) and assuming an ideal mixing behavior for the drug/lipid system, which implies additivity of the molecular area of the components. The calculations were performed as follows: the incorporation of the drug molecules into the lipid films implies a lateral compression of the lipid components in order to generate a free area, which in turn results in the observed  $\pi$  increase (reaching  $\pi_{eq}$  at long times). The vacant area was determined from the isotherms of the pure lipids (area change from 30 mN/m to  $\pi_{eq}$ ), and the amount of incorporated drug was determined as the fraction of drug that occupied this area from the isotherms of pure drug ( $X_{ASC_n}^{req}$ , see Section 5 in SI). Table 1 shows that this parameter also indicates a higher uptake capacity for POPC than for the more condensed films (SM16 and DSPC). However, different than  $X_{90}$ , the  $X_{ASC_n}^{req}$  does not show differences on the uptake capacity for the two analyzed drugs. This discrepancy may reflect some deviation of the ideality in the ASC<sub>*n*</sub>/lipid system, which is not considered in the  $X_{ASC_n}^{req}$  estimation but it is present in the surface titration method.

Taking them together, the data in Table 1 suggests that a small amount of ASC<sub>*n*</sub> may be responsible for the observed  $\pi$  increase of 26–27 mN/m in DSPC monolayers, while it would be necessary to incorporate a much larger amount of ASC<sub>*n*</sub> to POPC films to reach even a lesser increase in  $\pi$  (13–14 mN/m) (Table 1). Then, the resultant  $\pi_{eq}$  after drug incorporation appears as a weighted combination of both the drug uptake capacity and the response of the lipid films to such incorporation.

On the other hand, the Cho-containing films showed a moderate  $\pi$  increase (compared to DSPC) after ASC<sub>*n*</sub> penetration (15–18 mN/m), independent of whether the films behave as LO or LC phases, regarding their fluidity. This

fact may be explained by a very scarce  $ASC_n$  uptake capacity ( $X_{90} \leq 0.07$  and  $X_{ASC_n}^{req}$  from 0.03 to 0.17) for the three lipid films explored (pure Cho, CCM, and SCM).

The drug incorporation process might be related to the energy required to disrupt the attractive intermolecular lipid–lipid (van der Waals) interactions in order to introduce a new molecule (drug) to the film. This intermolecular forces, traditionally expressed as “cohesive pressure”<sup>33</sup> depends on the phase state of the film in the order  $S > LC > LE > G \sim 0$  and has been proposed to be very high for Cho-containing membranes.<sup>38</sup> Table 1 shows roughly an inverse correlation between the  $Cs^{-1}$  of lipid films and their capacity of incorporate  $ASC_n$  ( $X_{90}$  and  $X_{ASC_n}^{req}$ ), regardless their diffusional properties. The  $Cs^{-1}$  parameter reflects the lipid–lipid cohesion forces since highly incompressible phases are the result of a compact and cohesive molecular arrangement.

Additionally, a lowering in the  $Cs^{-1}$  value due to the  $ASC_n$  incorporation (as shown in Figure 4D) evidences a loss in the condensed character and in the cohesion intermolecular forces, likely lowering the activation energy for insertion of new drug molecules once a given amount has already been incorporated. Then, this process appeared to be cooperative, and the described modulation of the compressional properties is probably one of the reasons for the previously observed biphasic kinetic character of the  $ASC_n$  incorporation into lipid monolayers (see Figure 4A and ref 5).

#### 4. CONCLUSIONS

The  $ASC_n$  family has been used in different pharmacological preparations due to its amphiphilic nature. All these applications indirectly imply the interaction of  $ASC_n$  with cell membranes and/or stratum corneum. The length of the acyl chain (acting as the hydrophobic tail) of the  $ASC_n$  compounds subtly regulates the effectiveness of those pharmacological applications. We previously demonstrated that those chemical differences have large implications in the surface activity and in-plane organization of the  $ASC_n$  films.<sup>4</sup> In the present work, we also demonstrated that these differences in the chemical structures of the  $ASC_n$  induces differential changes in the physico-chemical properties of the host lipid membrane and regulate the extent of incorporation and the kinetics of the penetration process (see Figure 4 and Table 1).

Our results allow a breakthrough in the understanding of the relationship between the  $\pi_{eq}$  and the drug uptake capacity. For drugs, as well as for amphitropic proteins, penetration experiments have been used to estimate their affinity for membranes, but an obscure relationship between the  $\pi$  increase and the amount of protein at the interface has prevailed along time.<sup>48,51</sup> Our work strongly suggests that the  $\pi$  increase after the incorporation of an amphiphile into the lipid membrane has not a linear relationship with the incorporation extent of such amphiphile in the surface but this relationship is strongly influenced by the compressibility properties of the film. Then, the resultant observable  $\pi$  increase is a function of the capacity to incorporate such amphiphile as well as the response of the film upon a dilatational stress. As a result, monolayers that show S or LC phase state will respond with a larger  $\pi$  increase to the incorporation of a comparable amount of amphiphiles than LE ones. Additionally, the compressibility properties of the films also may be altered by the amphiphile incorporation, as in the case described here.

The present work provides a first approach to the understanding of membrane susceptibility to amphiphile

penetration, taking the  $ASC_n$  family as model because it represents an extremely efficient membrane perturber.<sup>4</sup> Our results indicate a higher susceptibility of  $ASC_n$  uptake for membranes in the liquid-expanded phase state (the main phase state proposed for cell membranes) than in more condensed ones or those with high content of Cho. This suggest that the Cho content in different cell membranes may set the bases of cell selectivity for drug incorporation.

A restriction of drug incorporation into membranes induced by the presence of Cho has been repetitively reported for different drug/membrane systems.<sup>22–25</sup> A detailed computational simulation study about drug permeation through lipid bilayers<sup>26</sup> concludes that, as has been early suggested by Kinnunen and co-workers,<sup>25</sup> the high lateral lipid packing induced by Cho<sup>38</sup> may be responsible of an inhibited incorporation capacity for small hydrophobic drugs into the hydrophobic core of the membrane. This condensation effect of Cho on phospholipid membranes has been known since early PC/Cho monolayer studies by McConnell<sup>34</sup> and later extended for other lipids.<sup>38</sup>

The SCM films with both a condensed character and high content of Cho shows scarce  $ASC_n$  uptake capacity, which is in accordance with the barrier function of stratum corneum. Then, our study suggests an important contribution of Cho in the maintenance of the barrier function of the stratum corneum. As stated by Bloom and Mouritsen in “The evolution of membranes”,<sup>12</sup> the presence of Cho in eukaryotic cell membranes may respond to the evolutionary pressure of an increasing amount of  $O_2$  in the atmosphere. Then, the incorporation of Cho into cell membranes increased membrane thickness adding mechanical strength and reducing the permeability of membranes.<sup>12</sup> In a similar way, the presence of Cho in stratum corneum, besides reducing the loss of  $H_2O$  and the incorporation of  $O_2$  to the organism may also provide a lesser susceptibility to incorporate amphiphilic molecules from the media.

In conclusion, our work highlights the preponderance of the compression properties of the membrane over the diffusional properties as the physical characteristics that regulate drug incorporation into model membranes. This is not an a priori obvious finding and as far as we know this is the first study focused on this aspect of membrane-amphiphilic drug interaction, taking the drug-membrane system not from a molecular point of view but as a soft matter system.

#### ■ ASSOCIATED CONTENT

##### 📄 Supporting Information

The Supporting Information is available free of charge on the ACS Publications website at DOI: 10.1021/acs.langmuir.5b04175.

Surface pressure -area isotherms; diffusion coefficient of microspheres on lipid monolayers of different rheological characteristics; Brewster angle microscopy; penetration of  $ASC_{16}$  and  $ASC_{14}$  into phospholipid monolayers; Estimation of the  $ASC_n$  mole fraction at equilibrium pressure in penetration experiments; and additional references. (PDF)

#### ■ AUTHOR INFORMATION

##### Corresponding Author

\*E-mail: lfanani@fcq.unc.edu.ar.



## Notes

The authors declare no competing financial interest.

## ACKNOWLEDGMENTS

This work was supported by the Consejo Nacional de Investigaciones Científicas y Técnicas (CONICET), Agencia Nacional de Promoción Científica y Tecnológica (ANPCyT, FONCyT PICT 2012-0344, PICT 2013-1175 and PICT 2014-1627), and the Secretary of Science and Technology of Universidad Nacional de Córdoba (SECyT-UNC), Argentina. At the present, M.M. is a doctoral student at Instituto de Investigaciones Biológicas y Tecnológicas (IByT), CONICET-UNC, Depto. de Química, FCEfYn. Y.M.Z.D. and M.M. are CONICET fellows and R.V.V., N.W., and M.L.F. are Career Investigators of CONICET-UNC.

## ABBREVIATIONS:

ASC<sub>n</sub>, L-ascorbic acid alkyl esters; ASC<sub>16</sub>, ascorbyl palmitate; ASC<sub>14</sub>, ascorbyl myristate; POPC, 1-palmitoyl-2-oleoyl-*sn*-glycero-3-phosphocholine; DSPC, 1,2-distearoyl-*sn*-glycero-3-phosphocholine; SM16, *N*-palmitoyl-*D*-erythro-sphingosylphosphorylcholine; Cho, cholesterol; ChoS, cholesterol 3-sulfate sodium salt; Cer24, *N*-lignoceroyl-*D*-erythro-sphingosine; CRM, cholesterol-rich membrane; SCM, stratum corneum mimicking membrane; LA, lignoceric acid; LE, liquid-expanded phase; LC, liquid-condensed phase; LO, liquid-ordered phase; S, solid phase;  $\pi$ , surface pressure; Cs<sup>-1</sup>, compressibility modulus; MMA, mean molecular area; BAM, Brewster angle microscopy; MSD, mean-square displacement

## REFERENCES

- (1) Palma, S.; Manzo, R. H.; Allemandi, D.; Fratoni, L.; Lo Nostro, P. Coagels from Ascorbic Acid Derivatives. *Langmuir* **2002**, *18* (24), 9219–9224.
- (2) Palma, S.; Manzo, R.; Lo Nostro, P.; Allemandi, D. Nanostructures from Alkyl Vitamin C Derivatives (ASCn): Properties and Potential Platform for Drug Delivery. *Int. J. Pharm.* **2007**, *345* (1–2), 26–34.
- (3) Benedini, L.; Fanani, M. L.; Maggio, B.; Wilke, N.; Messina, P.; Palma, S.; Schulz, P. Surface Phase Behavior and Domain Topography of Ascorbyl Palmitate Monolayers. *Langmuir* **2011**, *27* (17), 10914–10919.
- (4) Mottola, M.; Vico, R. V.; Villanueva, M. E.; Fanani, M. L. Alkyl Esters of L-Ascorbic Acid: Stability, Surface Behaviour and Interaction with Phospholipid Monolayers. *J. Colloid Interface Sci.* **2015**, *457*, 232–242.
- (5) Mottola, M.; Wilke, N.; Benedini, L.; Oliveira, R. G.; Fanani, M. L. Ascorbyl Palmitate Interaction with Phospholipid Monolayers: Electrostatic and Rheological Preponderancy. *Biochim. Biophys. Acta, Biomembr.* **2013**, *1828* (11), 2496–2505.
- (6) Tártara, L. I.; Quinteros, D. a.; Saino, V.; Allemandi, D. a.; Palma, S. D. Improvement of Acetazolamide Ocular Permeation Using Ascorbyl Laurate Nanostructures as Drug Delivery System. *J. Ocul. Pharmacol. Ther.* **2012**, *28* (2), 102–109.
- (7) Saino, V.; Monti, D.; Buralassi, S.; Tampucci, S.; Palma, S.; Allemandi, D.; Chetoni, P. Optimization of Skin Permeation and Distribution of Ibuprofen by Using Nanostructures (coagels) Based on Alkyl Vitamin C Derivatives. *Eur. J. Pharm. Biopharm.* **2010**, *76* (3), 443–449.
- (8) Sánchez Vallecillo, M. F.; Ullio Gamboa, G. V.; Palma, S. D.; Harman, M. F.; Chiodetti, A. L.; Morón, G.; Allemandi, D. a.; Pistoresi-Palencia, M. C.; Maletto, B. a. Adjuvant Activity of CpG-ODN Formulated as a Liquid Crystal. *Biomaterials* **2014**, *35* (8), 2529–2542.
- (9) Benedini, L.; Antollini, S.; Fanani, M. L.; Palma, S.; Messina, P.; Schulz, P. Study of the Influence of Ascorbyl Palmitate and

Amiodarone in the Stability of Unilamellar Liposomes. *Mol. Membr. Biol.* **2014**, *31* (2–3), 85–94.

(10) Kharrat, N.; Aissa, I.; Sghaier, M.; Bouaziz, M.; Sellami, M.; Laouini, D.; Gargouri, Y. *J. Agric. Food Chem.* **2014**, *62*, 9118.

(11) Bouwstra, J. A.; Honeywell-Nguyen, P. L.; Gooris, G. S.; Ponec, M. Structure of the Skin Barrier and Its Modulation by Vesicular Formulations. *Prog. Lipid Res.* **2003**, *42* (1), 1–36.

(12) Mouritsen, O. G.; Bloom, M. The Evolution of Membranes. In *Handbook of Biological Physics*; Lipowsky, R., Sackmann, E., Eds.; Elsevier Science: Amsterdam, 1995; Vol. 1, pp 65–95.

(13) Bouwstra, J. a.; Honeywell-Nguyen, P. L.; Gooris, G. S.; Ponec, M. Structure of the Skin Barrier and Its Modulation by Vesicular Formulations. *Prog. Lipid Res.* **2003**, *42* (1), 1–36.

(14) Garza, A.; López-Ramírez, O.; Vega, R.; Soto, E.; Kessner, D.; Ruettinger, a.; Kiselev, M. a.; Wartewig, S.; Neubert, R. H. H.; Eeman, M.; et al. Properties of Ceramides and Their Impact on the Stratum Corneum Structure: A Review - Part 2: Stratum Corneum Lipid Model Systems. *Skin Pharmacol. Physiol.* **2008**, *25* (2), 3029–3039.

(15) Mercado, F. V.; Maggio, B.; Wilke, N. Phase Diagram of Mixed Monolayers of Stearic Acid and Dimyristoylphosphatidylcholine. Effect of the Acid Ionization. *Chem. Phys. Lipids* **2011**, *164* (5), 386–392.

(16) Fanani, M. L.; Maggio, B. Phase State and Surface Topography of Palmitoyl-Ceramide Monolayers. *Chem. Phys. Lipids* **2010**, *163* (6), 594–600.

(17) López-Montero, I.; Catapano, E. R.; Espinosa, G.; Arriaga, L. R.; Langevin, D.; Monroy, F. Shear and Compression Rheology of Langmuir Monolayers of Natural Ceramides: Solid Character and Plasticity. *Langmuir* **2013**, *29* (22), 6634–6644.

(18) Espinosa, G.; López-Montero, I.; Monroy, F.; Langevin, D. Shear Rheology of Lipid Monolayers and Insights on Membrane Fluidity. *Proc. Natl. Acad. Sci. U. S. A.* **2011**, *108* (15), 6008–6013.

(19) Fanani, M. L.; Maggio, B. Liquid-Liquid Domain Miscibility Driven by Composition and Domain Thickness Mismatch in Ternary Lipid Monolayers. *J. Phys. Chem. B* **2011**, *115* (1), 41–49.

(20) Školová, B.; Januššová, B.; Zbytovská, J.; Gooris, G.; Bouwstra, J.; Slepíčka, P.; Berka, P.; Roh, J.; Palát, K.; Hrabálek, A.; et al. Ceramides in the Skin Lipid Membranes: Length Matters. *Langmuir* **2013**, *29* (50), 15624–15633.

(21) Ten Grotenhuis, E.; Demel, R. a.; Ponec, M.; Boer, D. R.; van Miltenburg, J. C.; Bouwstra, J. a. Phase Behavior of Stratum Corneum Lipids in Mixed Langmuir-Blodgett Monolayers. *Biophys. J.* **1996**, *71* (3), 1389–1399.

(22) Gzyl-Malcher, B.; Handzlik, J.; Klekowska, E. Temperature Dependence of the Interaction of Prazosin with Lipid Langmuir Monolayers. *Colloids Surf, B* **2013**, *112*, 171–176.

(23) Fadel, O.; El Kirat, K.; Morandat, S. The Natural Antioxidant Rosmarinic Acid Spontaneously Penetrates Membranes to Inhibit Lipid Peroxidation in Situ. *Biochim. Biophys. Acta, Biomembr.* **2011**, *1808* (12), 2973–2980.

(24) Zhao, L.; Feng, S. S. Effects of Cholesterol Component on Molecular Interactions between Paclitaxel and Phospholipid within the Lipid Monolayer at the Air-Water Interface. *J. Colloid Interface Sci.* **2006**, *300* (1), 314–326.

(25) Söderlund, T.; Lehtonen, J. Y.; Kinnunen, P. K. Interactions of Cyclosporin A with Phospholipid Membranes: Effect of Cholesterol. *Mol. Pharmacol.* **1999**, *55* (1), 32–38.

(26) Yacoub, T. J.; Reddy, A. S.; Szleifer, I. Structural Effects and Translocation of Doxorubicin in a DPPC/Chol Bilayer: The Role of Cholesterol. *Biophys. J.* **2011**, *101* (2), 378–385.

(27) Gaines, G. L. *Insoluble Monolayers*; Prigogine, I., Ed.; Interscience Publishers: New York, 1968.

(28) Wilke, N.; Vega Mercado, F.; Maggio, B. Rheological Properties of a Two Phase Lipid Monolayer at the Air/water Interface: Effect of the Composition of the Mixture. *Langmuir* **2010**, *26* (13), 11050–11059.

(29) Vollhardt, D. Brewster Angle Microscopy: A Preferential Method for Mesoscopic Characterization of Monolayers at the Air/



water Interface. *Curr. Opin. Colloid Interface Sci.* **2014**, *19* (3), 183–197.

(30) Lheveder, C.; Meunier, J. Brewster Angle Microscopy. In *Physical Chemistry of Biological Interfaces*; Baszkin, A., Norde, W., Eds.; Marcel Dekker, Inc.: New York, 2000.

(31) Smaby, J. M.; Momsen, M. M.; Brockman, H. L.; Brown, R. E. Phosphatidylcholine Acyl Unsaturation Modulates the Decrease in Interfacial Elasticity Induced by Cholesterol. *Biophys. J.* **1997**, *73* (3), 1492–1505.

(32) Li, X. M.; Smaby, J. M.; Momsen, M. M.; Brockman, H. L.; Brown, R. E. Sphingomyelin Interfacial Behavior: The Impact of Changing Acyl Chain Composition. *Biophys. J.* **2000**, *78* (4), 1921–1931.

(33) Davies, J. T.; Rideal, E. K. *Interfacial Phenomena*; Academic Press: London, 1963.

(34) McConnell, H. M.; Radhakrishnan, A. Condensed Complexes of Cholesterol and Phospholipids. *Biochim. Biophys. Acta, Biomembr.* **2003**, *1610* (2), 159–173.

(35) Mattjus, P.; Slotte, J. P. Does Cholesterol Discriminate between Sphingomyelin and Phosphatidylcholine in Mixed Monolayers Containing Both Phospholipids? *Chem. Phys. Lipids* **1996**, *81* (1), 69–80.

(36) Joos, P. Cholesterol as Liquifier In Phospholipid Membranes Studied by Surface Viscosity Measurements of Mixed Monolayers. *Chem. Phys. Lipids* **1970**, *4*, 162–168.

(37) McMullen, T. P. W.; Lewis, R. N. a H.; McElhaney, R. N. Cholesterol-Phospholipid Interactions, the Liquid-Ordered Phase and Lipid Rafts in Model and Biological Membranes. *Curr. Opin. Colloid Interface Sci.* **2004**, *8* (6), 459–468.

(38) Quinn, P. J.; Wolf, C. The Liquid-Ordered Phase in Membranes. *Biochim. Biophys. Acta, Biomembr.* **2009**, *1788* (1), 33–46.

(39) Fisher, T.; Dhar, P.; Heinig, P. The Viscous Drag of Spheres and Filaments Moving in Membranes or Monolayers. *J. Fluid Mech.* **2006**, *558*, 451–475.

(40) Sickert, M.; Rondelez, F.; Stone, H. a. Single-Particle Brownian Dynamics for Characterizing the Rheology of Fluid Langmuir Monolayers. *Europhys. Lett.* **2007**, *79* (6), 66005.

(41) De Almeida, R. F. M.; Fedorov, A.; Prieto, M. Sphingomyelin/phosphatidylcholine/cholesterol Phase Diagram: Boundaries and Composition of Lipid Rafts. *Biophys. J.* **2003**, *85* (4), 2406–2416.

(42) Edidin, M. The State of Lipid Rafts: From Model Membranes to Cells. *Annu. Rev. Biophys. Biomol. Struct.* **2003**, *32*, 257–283.

(43) McConnell, H. M. Structures and Transitions in Lipid Monolayers at the Air-Water Interface. *Annu. Rev. Phys. Chem.* **1991**, *42* (1), 171–195.

(44) Busto, J. V.; Fanani, M. L.; De Tullio, L.; Sot, J.; Maggio, B.; Goñi, F. M.; Alonso, A. Coexistence of Immiscible Mixtures of Palmitoylsphingomyelin and Palmitoylceramide in Monolayers and Bilayers. *Biophys. J.* **2009**, *97* (10), 2717–2726.

(45) Kubo, I.; Adachi, S.; Maeda, H.; Seki, A. Phosphatidylcholine Monolayers Observed with Brewster Angle Microscopy and  $\Pi$ -A Isotherms. *Thin Solid Films* **2001**, *393* (1–2), 80–85.

(46) Eeman, M.; Francius, G.; Dufrene, Y. F.; Nott, K.; Paquot, M.; Deleu, M. Effect of Cholesterol and Fatty Acids on the Molecular Interactions of Fengycin with Stratum Corneum Mimicking Lipid Monolayers. *Langmuir* **2009**, *25* (5), 3029–3039.

(47) Mangiarotti, A.; Wilke, N. Energetics of the Phase Transition in Free-Standing versus Supported Lipid Membranes. *J. Phys. Chem. B* **2015**, *119* (28), 8718–8724.

(48) Maget-Dana, R. The Monolayer Technique: A Potent Tool for Studying the Interfacial Properties of Antimicrobial and Membrane-Lytic Peptides and Their Interactions with Lipid Membranes. *Biochim. Biophys. Acta, Biomembr.* **1999**, *1462* (2), 109–140.

(49) Marsh, D. Lateral Pressure in Membranes. *Biochim. Biophys. Acta, Rev. Biomembr.* **1996**, *1286* (3), 183–223.

(50) Demel, R. a.; Geurts van Kessel, W. S.; Zwaal, R. F.; Roelofs, B.; van Deenen, L. L. Relation between Various Phospholipase Actions on Human Red Cell Membranes and the Interfacial Phospholipid

Pressure in Monolayers. *Biochim. Biophys. Acta, Biomembr.* **1975**, *406* (1), 97–107.

(51) Peetla, C.; Stine, V. L. Biophysical Interactions with Model Lipid Membranes: Applications in Drug Discovery and Drug Delivery. *Mol. Pharmaceutics* **2009**, *6* (5), 1264–1276.